

# Fault activity and lateral extrusion inferred from velocity field revealed by GPS measurements in the Pingtung area of southwestern Taiwan

Jyr-Ching Hu <sup>a,\*</sup>, Chin-Shyong Hou <sup>b</sup>, Li-Chung Shen <sup>a</sup>, Yu-Chang Chan <sup>c</sup>,  
Rou-Fei Chen <sup>d</sup>, Chung Huang <sup>a</sup>, Ruey-Juin Rau <sup>e</sup>, Kate Hui-Hsuan Chen <sup>e</sup>,  
Chii-Wen Lin <sup>b</sup>, Mong-Han Huang <sup>a</sup>, Pei-Fen Nien <sup>a</sup>

<sup>a</sup> Department of Geosciences, National Taiwan University, No. 1, Sec. 4, Roosevelt Road, Taipei 106, Taiwan

<sup>b</sup> Central Geological Survey, MOEA, PO Box 968, Taipei, Taiwan

<sup>c</sup> Institute of Earth Sciences, Academia Sinica, Nankang, Taiwan

<sup>d</sup> Observatoire Océanologique de Villefranche-sur-Mer, Université P.&M. Curie, Villefranche-sur-Mer, France

<sup>e</sup> Department of Earth Sciences, National Cheng Kung University, Tainan, Taiwan

Received 5 May 2004; received in revised form 18 February 2005; accepted 27 July 2006

## Abstract

Four campaigns of dense GPS measurements have been conducted since 1995 to investigate crustal deformation patterns in SW Taiwan. The station velocities decrease westwards from 42.2 to 55.5 mm/yr along the azimuths from 247.1° to 272.5°. In central part of the study area, GPS stations move nearly toward the west, whereas in the Pingtung–Kaohsiung coastal area, displacement vectors demonstrate a clear counter-clockwise deviation toward the SW. The transtensional deformation and the along-strike variation of southward increase of extensional deformation is due to the low lateral confining conditions related to the Manila subduction zone as a free boundary or/and the presence of the prominent Peikang High as a rigid indenter. The Chishan Fault is dominated by right-lateral motion with a fault slip rate  $\sim 7$  mm/yr in a N50°W direction. The Kaoping Fault is dominated by left-lateral motion with a  $\sim 4$ –8 mm/yr in a N–S direction. The significant right-lateral component of motion of  $\sim 24$ –30 mm/yr is accommodated along the active structures west of the Chishan Fault. The right-lateral and left-lateral structures facilitate the southwestward extrusion. The velocity gradients of the GPS stations across the Chaochou Fault are not significant. This implies that the Chaochou Fault is locked along the fault plane.

© 2006 Elsevier Ltd. All rights reserved.

**Keywords:** GPS; Crustal deformation; Active fault; Taiwan

## 1. Introduction

Space geodetic techniques, especially the global position system (GPS), have become a powerful tool for high accuracy geodetic monitoring of a wide range of geophysical phenomena such as plate motion, deformation associated with earthquakes and volcanoes, fault activity and crustal deformation at plate boundaries (Dixon, 1991; Segall and Davis, 1997). In order to quantify the kinematics of defor-

mation along the convergent plate boundary of Taiwan, the “Taiwan GPS Network” was established in 1990 with dual-frequency geodetic receivers (Yu et al., 1997; Yu and Kuo, 2001; Hickman et al., 2002). These data provided the amplitude and orientation of tectonic motion across the plate boundary of Taiwan, and hence direct constraints on geodynamics. Some limitations in the direct interpretation of such studies were later highlighted by the co-seismic deformation of the Chichi earthquake. This major earthquake clearly revealed that the inter-seismic deformation documented by the brevity of GPS surveys did not provide a complete picture of the deformation across the collision belt. The long-term deformation pattern includes a major

\* Corresponding author. Tel.: +886 2 23634860; fax: +886 2 23636095.  
E-mail address: [jchu@ntu.edu.tw](mailto:jchu@ntu.edu.tw) (J.-C. Hu).

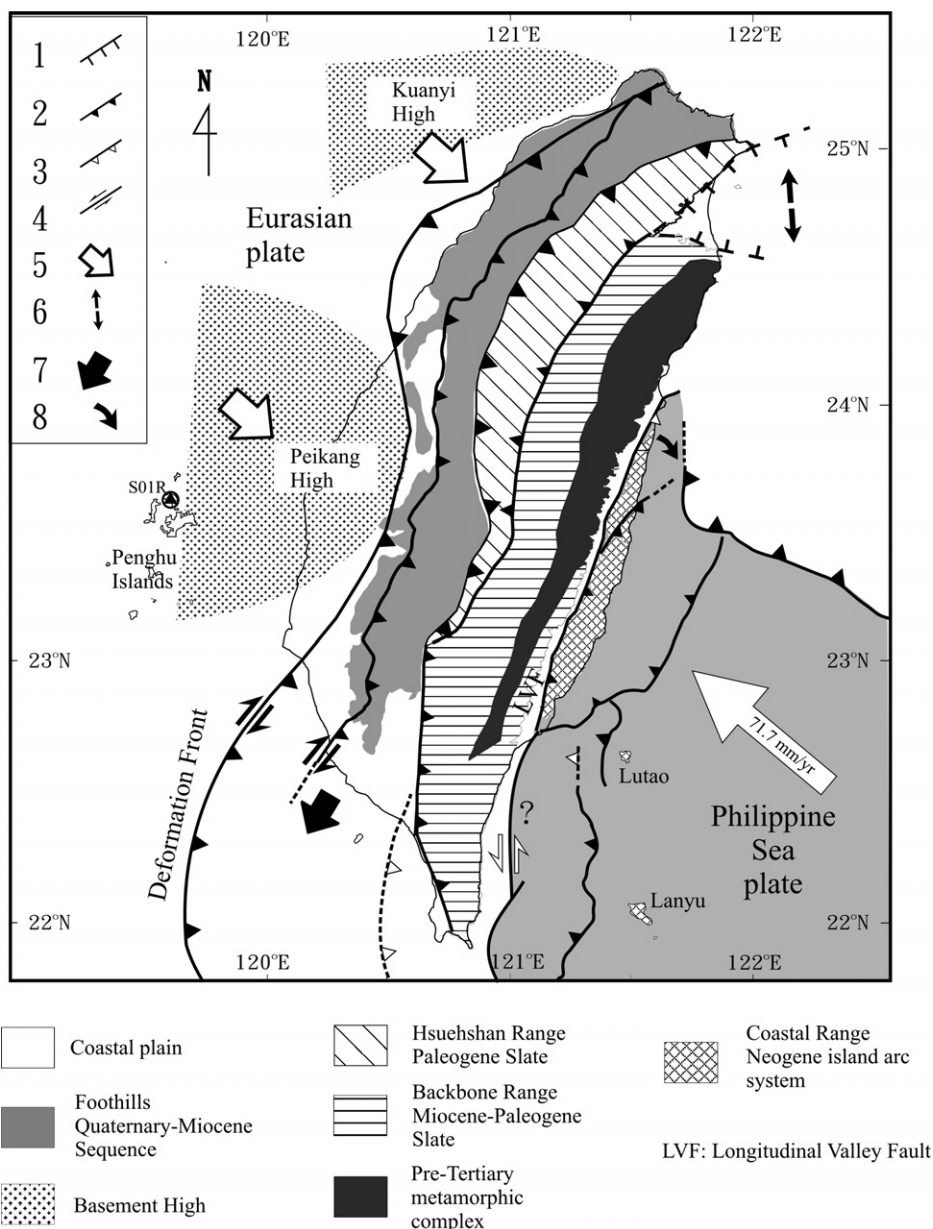


Fig. 1. Tectonic framework and main structural units in Taiwan (modified after Teng, 1990; Hu et al., 2001; Lacombe et al., 2001; Malavieille et al., 2002). Large Open arrow shows the direction and velocity of plate convergence of Philippine Sea plate and Eurasian plate relative to the South China block (Yu et al., 1997, 1999). Major thrust faults with triangles are on the upthrust side. Numbers indicate 1, normal fault; 2, thrust fault (active); 3, thrust fault (inactive); 4, strike-slip fault; 5, indenter of rigid promontory at the front of the active belt; 6, back-arc opening; 7, tectonic escape; 8, migration of the thrust front.

co-seismic component of deformation, which dominates near front of the belt and highlights a double plate boundary structure (Angelier et al., 2001). A further limitation of the initial Taiwan GPS Network involved sparse coverage of GPS stations in some areas was less than comprehensive and did not permit detailed reconstruction of the deformation. This was the case in the Pingtung plain, although GPS data suggested a different present-day deformation, as compared with northern regions close to the front of the belt. To better reconstruct the ongoing deformation, a dense network was established since 1996 in the Kaohsiung and Pingtung areas. It thus became possible to monitor the crustal deformation along and around major crustal

structures such as the Chaochou Fault and the Chishan Fault (Fig. 1).

The still ongoing collision between the Luzon volcanic arc and the China continental margin of Eurasian plate began ca. 5 Ma (e.g., Chai, 1972; Suppe, 1984; Angelier, 1986; Ho, 1986; Teng, 1990, 1996). This collision belt connects the Ryukyu subduction zone, where Philippine Sea plate is subducting beneath the Eurasian plate, and the Manila subduction zone, where the Philippine Sea plate is overriding the crust of South China Sea (Fig. 1). The GPS measurements and the NUVEL-1 and-1A models of global plate motion predict motion of the Philippine Sea plate toward the northwest ( $\sim 305\text{--}310^\circ$ ), at a rate of

70–82 mm/yr relative to the Eurasia plate, in good directional agreement with, but at a greater velocity than the previous estimates (Seno et al., 1993; Yu et al., 1997, 1999; Zang et al., 2002). Based on geological and seismological evidence, the NNE trending Longitudinal Valley Fault is considered to be the major suture zone between the two plates (Ho, 1986; Tsai, 1986). However, field measurements of the fault displacement suggested and consideration of major thrust events to the west confirmed that it accommodates no more than 25–30% of the total convergence across the Taiwan collision belt (Angelier et al., 2000, 2001). Furthermore, the trend of the relative plate-motion vector undergoes a 15–20° clockwise deviation as compared with the direction perpendicular to the structural grain of the orogenic belt, indicating a significant left-lateral component of motion. In response to this obliquity, the orogenic belt propagates southward at a rate of ~55 km/my (Suppe, 1984; Byrne and Crespi, 1997). The collision is no longer active in northernmost Taiwan and the transtensional tectonic regime prevails due to different mechanical processes (Hu and Angelier, 1996; Hu et al., 1996, 2002; Teng, 1996). The orogenic belt of central-southern Taiwan is undergoing strong crustal deformation (Yu and Chen, 1994; Yu et al., 1997), rapid uplift (Liew et al., 1990; Liu and Yu, 1990; Wang and Burnett, 1990; Pirazzoli et al., 1993; Chen and Liu, 2000; Vita-Finzi, 2000; Liu et al., 2001) and high denudation and erosion rate (Li, 1976; Hovius et al., 2000; Dadson et al., 2003) in a typical compressional regime. In this paper, we discuss the tectonic behavior near the southern tip of the Taiwan belt, close to the transition zone between the mountain ranges of the collision zone and the submarine accretionary prism of the northern Manila subduction zone.

The theory of lateral extrusion along a collision zone has been documented over more than two decades ago (Molnar and Tapponnier, 1978; Tapponnier et al., 1983; Ratschbacher et al., 1991). The basic concept of tectonic extrusion refers to the lateral motion of a structural unit that moves toward a free boundary in response to collision shortening. Its application to SW Taiwan deserves discussion because it is usually considered over larger areas and generally occurs at crustal-lithospheric scales along major transcurrent faults. Southwestern Taiwan is a region where lateral extrusion is expected because it is the transition zone between the collision belt and the offshore Manila subduction zone. In more detail, this lateral extrusion is also related to both the collisional shortening and the indentation of the Peikang basement high (Fig. 1). Sandbox modeling supported the interpretation of southwestern Taiwan undergoing tectonic extrusion toward the SW (Lu and Malavieille, 1994; Lu et al., 1998). The relationship between the kinematic evolution of the fold-and-thrust units of the southwestern Foothills and the offshore accretionary prism is a key topic for understanding the crustal deformation and mechanical behavior of this transition zone. The aim of this study is to examine this lateral extrusion hypothesis and the fault activity of the Pingtung area in SW Taiwan primarily based

on the results of new dense GPS network data gathered from 1996 to 1999.

## 2. Tectonic and geological background of Pingtung area

Southwestern Taiwan is located on a transition zone between collision and subduction and corresponds to the southern part of the Plio-Pleistocene foreland basin in response to lithospheric flexure due primarily to the tectonic loading of the Central Range (Lin and Watts, 2002). The Western Foothills of Taiwan are composed of a series of imbricated folds and thrust sheets affected by basement-involved tectonics (Mouthereau et al., 2002). The Pingtung plain, which covers an area of 1210 km<sup>2</sup>, exhibits a rectangular shape when mapped and viewed in cross section display fills of unconsolidated sediments of the late Pleistocene and the Holocene. Most of these sediments consist of coastal to estuarine sand and mud, with abundant shallow marine to lagoonal shells and foraminifers (Shyu, 1999; Chiang et al., 2004). The Pingtung plain is bounded by low hills of deformed Quaternary sediments to the north and the west and to the east, the plain is bounded by metamorphosed tertiary rocks of the Central Mountain Range. Based on a recent neotectonic map (Shyu et al., 2005), the Pingtung plain comprises the major element of a proposed “Kaoping domain” located between the outer-arc ridge sediments of the Central Range and the continental shelf deposits of the Western Foothills. The present-day Pingtung plain corresponds to the forearc domain between the trench to the west and the forearc ridge to the east. This more-than-100-km-wide domain has undergone major shortening and thus transformed into a fold-and-thrust belt of the Western Foothills of Taiwan. To the south, numerous anticlinal ridges and minor thrust faults on the seafloor indicate the initial shortening of this forearc space (Liu et al., 1997; Lundberg et al., 1997; Lacombe et al., 1999).

Active neotectonics has been investigated by morphological data in southwestern Taiwan (Bonilla, 1975, 1977; Hsu and Chang, 1979; Shyu et al., 2005). The most significant geomorphological feature of the Pingtung plain is the straight, N–S trending Chaochou Fault escarpment separating the alluvium plain and the high mountains (Fig. 2). East of the Chaochou Fault, the mountains are mainly composed of Eocene–Miocene argillite, slate and meta-sandstone. The contrast between rock ages and the difference in elevation between the two sides of the Chaochou Fault highlights a major vertical relative displacement. The remarkable straight shape of this fault line in the geological maps may suggest the existence of a significant component of strike-slip motion. Thus, the Chaochou Fault is considered as a probable oblique-slip fault zone that steeply dips to the east.

Recent studies have shown that the Chaochou Fault and its adjacent areas actually experienced transtensional tectonic movements (Chan et al., 2000). Based on tectonic analysis of outcrop-scale faults, a predominant transtensional tectonic regime with NNE to NE extension and ESE

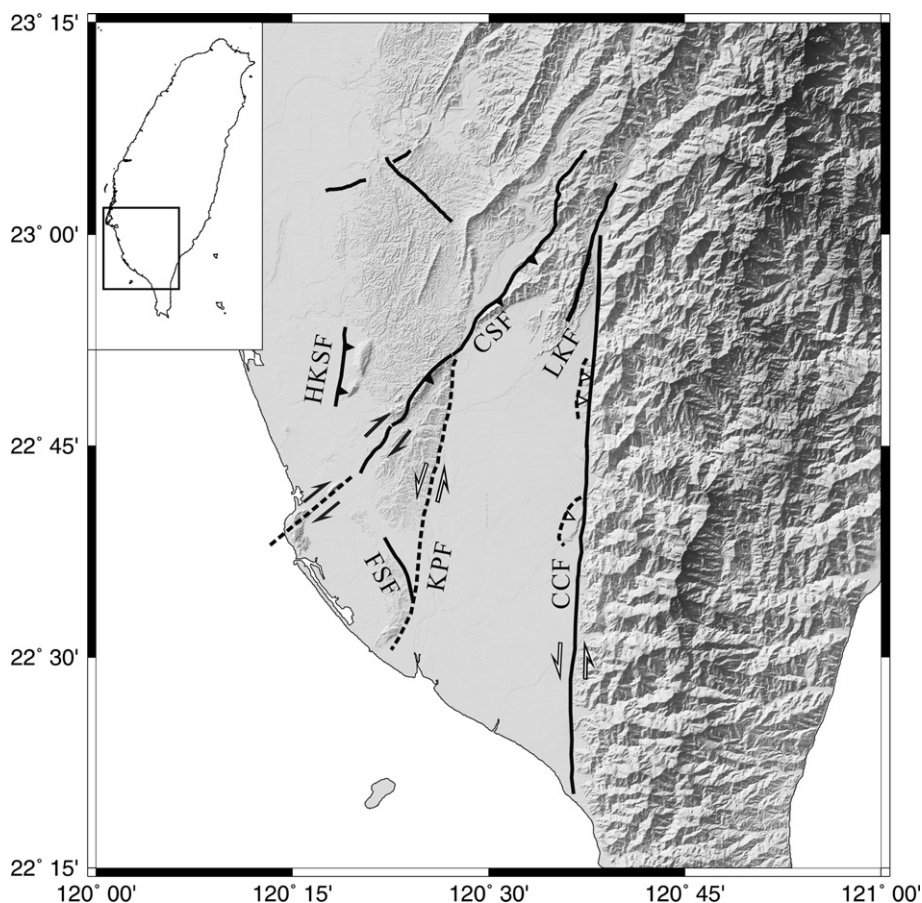


Fig. 2. Neotectonic map of southwestern Taiwan of the study area (modified after Shyu et al., 2005). Thick lines indicate the active faults (Lin et al., 2000). CCF, Chaochou Fault; CSF, Chishan Fault; LKF, Liukuei Fault; HKSF, Hsiaokangshan Fault; FSF, Fengshan Fault; and KPF, Kaoping Fault. The dashed line indicates the inferred fault. Inset shows the location of the study area.

to SE compression was reconstructed on the eastern side of the Chaochou Fault (Chan et al., 2000). The transition from transpression to recent transtension was also highlighted along the Chaochou Fault and is probably related to the transition from collision to subduction, which highlights the active extrusion of the study area towards the southeast. Within this geological framework, our geodetic (GPS) analysis aimed at a better characterization of the present-day deformation in the area.

### 3. The Pingtung GPS network

The 'Pingtung GPS Network' was established in 1995 by the Central Geological Survey, Ministry of Economic Affairs, to analyze present-day crustal deformation and land subsidence in the Pingtung area (Fig. 3). It is composed of 48 annually surveyed stations and one permanent, continuously monitoring station (S23R), covering the Pingtung and Kaohsiung area.

During the period from August 1995 to August 1999, the mobile stations of the network were surveyed 3–4 times with dual frequency geodetic GPS receivers. The changes in baseline components derived from these repeated and continuous GPS measurements provided accurate estimates of the

relative velocities of GPS stations in study area. In each survey, 4–8 stations were observed simultaneously with dual-frequency geodetic receivers (Trimble 4000 SSE Geodetic Surveyor). A station was usually occupied during more than two sessions, each session being composed of 6–14 h of GPS observations to all available satellites rising higher than a 15° angle of elevation. The sampling interval was 15 s. Daily solutions were computed for continuous GPS data. The ionosphere-free linear combination of observations at the L1 and L2 frequencies were employed as the basic observation for estimating the station coordinates and baseline solutions. We have processed the observed data with the official, final and precise ephemerides distributed by the IGS.

All available temporary measurements and continuous recordings of GPS data were processed with the Bernese GPS software (v.4.2) developed at the Astronomical Institute of the University of Berne (Hugentobler et al., 2001). The observed data in each epoch survey were processed session by session to obtain the baseline solutions for all combinations of any two stations in the same session. The scatter of series of GPS measurements taken over several years can be employed as an indicator of precision. This long-term repeatability shows the effects of slowly varying systematic errors due to propagation delay, multipath, or



Table 1  
Velocities of GPS stations in Pingtung area

Station	Lon. (°)	Long. (°)	$V_e$ (mm/yr)	$V_n$ (mm/yr)	V (mm/yr)	Azimuth (°)
CLIA	120.4324	22.8300	$-46.5 \pm 1.5$	$-8.5 \pm 1.5$	$47.2 \pm 1.4$	$259.7 \pm 1.6$
FONS	120.3817	22.5300	$-40.7 \pm 1.7$	$-17.3 \pm 1.7$	$44.2 \pm 2.5$	$247.0 \pm 1.6$
G001	120.4959	22.7817	$-46.7 \pm 1.7$	$-5.7 \pm 1.7$	$47.0 \pm 2.2$	$263.0 \pm 1.7$
G002	120.4425	22.7230	$-45.7 \pm 1.7$	$-6.6 \pm 1.7$	$46.2 \pm 2.2$	$261.8 \pm 1.6$
G003	120.6098	22.7020	$-50.0 \pm 1.4$	$-0.6 \pm 1.4$	$50.0 \pm 1.8$	$269.3 \pm 1.2$
G004	120.5646	22.6612	$-47.3 \pm 1.9$	$-1.3 \pm 1.8$	$47.3 \pm 2.3$	$268.4 \pm 1.8$
G005	120.5258	22.6213	$-49.1 \pm 1.8$	$-3.4 \pm 1.7$	$49.2 \pm 2.3$	$266.0 \pm 1.5$
G006	120.5943	22.5707	$-49.4 \pm 1.9$	$0.9 \pm 1.9$	$49.4 \pm 2.3$	$271.0 \pm 1.9$
G007	120.4667	22.6543	$-45.0 \pm 2.1$	$-6.8 \pm 2.0$	$45.5 \pm 2.6$	$261.4 \pm 2.0$
G010	120.5884	22.5085	$-49.3 \pm 1.5$	$-1.9 \pm 1.6$	$49.3 \pm 2.1$	$267.7 \pm 1.3$
G011	120.3930	22.5075	$-38.2 \pm 1.7$	$-18.0 \pm 1.9$	$42.2 \pm 2.6$	$244.7 \pm 1.6$
G012	120.4515	22.5241	$-42.0 \pm 1.7$	$-13.6 \pm 1.8$	$44.1 \pm 2.5$	$252.0 \pm 1.6$
G013	120.5512	22.4713	$-48.6 \pm 1.6$	$-4.77 \pm 1.7$	$48.8 \pm 2.2$	$264.4 \pm 1.5$
G014	120.4955	22.4572	$-49.6 \pm 1.7$	$-11.9 \pm 1.8$	$51.0 \pm 2.2$	$256.5 \pm 1.5$
G015	120.4948	22.4258	$-46.4 \pm 1.7$	$-18.3 \pm 1.7$	$49.8 \pm 2.3$	$248.4 \pm 1.5$
G016	120.4608	22.8346	$-45.3 \pm 1.6$	$-4.11 \pm 1.5$	$45.5 \pm 2.1$	$264.8 \pm 1.4$
G017	120.5983	22.8272	$-44.5 \pm 1.5$	$-2.5 \pm 1.4$	$44.5 \pm 2.2$	$266.8 \pm 1.3$
G018	120.6107	22.7907	$-50.7 \pm 1.7$	$-2.4 \pm 1.6$	$50.7 \pm 2.0$	$267.3 \pm 1.5$
G019	120.5758	22.7536	$-49.3 \pm 1.6$	$-1.6 \pm 1.6$	$49.4 \pm 2.1$	$268.1 \pm 1.5$
G020	120.4899	22.7356	$-48.5 \pm 1.7$	$-4.3 \pm 1.7$	$48.6 \pm 2.2$	$265.0 \pm 1.5$
G021	120.5069	22.6982	$-46.8 \pm 1.8$	$-3.8 \pm 1.8$	$47.0 \pm 2.3$	$265.3 \pm 1.7$
G022	120.3947	22.6057	$-40.0 \pm 1.5$	$-14.4 \pm 1.5$	$42.5 \pm 2.3$	$250.2 \pm 1.3$
G023	120.4686	22.6147	$-44.2 \pm 1.7$	$-6.0 \pm 1.7$	$44.6 \pm 2.4$	$262.3 \pm 1.6$
G024	120.5946	22.6305	$-48.2 \pm 1.7$	$-0.7 \pm 1.7$	$48.2 \pm 2.1$	$269.2 \pm 1.5$
G025	120.5660	22.6086	$-47.0 \pm 1.8$	$0.1 \pm 1.7$	$47.0 \pm 2.3$	$270.2 \pm 1.7$
G026	120.4251	22.5652	$-43.3 \pm 1.6$	$-8.4 \pm 1.7$	$44.1 \pm 2.3$	$259.1 \pm 1.5$
G027	120.5430	22.5344	$-46.8 \pm 1.9$	$-3.8 \pm 2.0$	$47.0 \pm 2.6$	$265.4 \pm 1.8$
G028	120.5123	22.5146	$-47.4 \pm 1.9$	$-4.7 \pm 2.0$	$47.6 \pm 2.5$	$264.3 \pm 1.8$
G029	120.6159	22.4229	$-47.4 \pm 1.4$	$-0.8 \pm 1.5$	$47.4 \pm 2.2$	$269.1 \pm 1.2$
G030	120.4553	22.4702	$-41.0 \pm 1.7$	$-18.8 \pm 1.7$	$45.1 \pm 2.4$	$245.4 \pm 1.5$
G031	120.5266	22.4263	$-51.8 \pm 1.7$	$-5.0 \pm 1.7$	$52.0 \pm 2.2$	$264.5 \pm 1.5$
G033	120.5952	22.4095	$-46.6 \pm 1.6$	$-1.1 \pm 1.7$	$46.6 \pm 2.3$	$268.6 \pm 1.4$
G034	120.5812	22.3704	$-45.1 \pm 1.8$	$-0.5 \pm 1.9$	$45.1 \pm 2.7$	$269.4 \pm 1.6$
G035	120.6209	22.3306	$-43.8 \pm 1.6$	$-0.9 \pm 1.7$	$43.8 \pm 2.5$	$268.9 \pm 1.3$
G048	120.5536	22.8994	$-45.8 \pm 2.0$	$-4.2 \pm 1.9$	$46.0 \pm 2.5$	$264.7 \pm 1.9$
G049	120.6646	22.8855	$-55.1 \pm 2.5$	$-6.49 \pm 1.8$	$55.5 \pm 2.6$	$263.3 \pm 1.8$
G050	120.6491	22.5274	$-47.3 \pm 1.9$	$-0.1 \pm 1.9$	$47.3 \pm 2.4$	$269.8 \pm 1.8$
G051	120.4799	22.5631	$-42.2 \pm 1.7$	$-4.5 \pm 1.8$	$42.5 \pm 2.6$	$263.9 \pm 1.6$
G052	120.6319	22.5907	$-50.7 \pm 1.9$	$1.4 \pm 1.8$	$50.7 \pm 2.3$	$271.6 \pm 1.8$
G054	120.6330	22.8191	$-48.9 \pm 1.8$	$-0.4 \pm 1.7$	$48.9 \pm 2.2$	$269.5 \pm 1.6$
0575	120.6557	22.4156	$-49.9 \pm 2.0$	$1.7 \pm 2.0$	$49.9 \pm 2.5$	$271.9 \pm 1.9$
S23R	120.6061	22.6449	$-49.9 \pm 1.0$	$2.1 \pm 1.0$	$49.9 \pm 1.6$	$272.5 \pm 0.6$
I042	120.2446	22.7718	$-17.9 \pm 1.6$	$-2.1 \pm 1.6$	$18.0 \pm 1.6$	$263.3 \pm 1.6$
I045	120.3194	22.6694	$-42.4 \pm 1.8$	$-21.2 \pm 1.6$	$47.4 \pm 1.8$	$243.4 \pm 1.6$
LIUC	120.3707	22.3427	$-41.9 \pm 2.9$	$-14.7 \pm 3.2$	$44.4 \pm 2.9$	$250.7 \pm 3.2$
0621	120.4258	22.7915	$-45.6 \pm 1.4$	$-7.8 \pm 1.5$	$46.3 \pm 1.4$	$260.3 \pm 1.5$
S010	120.3718	22.5254	$-37.3 \pm 3.0$	$-17.1 \pm 2.0$	$41.0 \pm 2.8$	$245.4 \pm 2.2$
S022	120.6157	22.3683	$-48.2 \pm 2.2$	$5.3 \pm 2.3$	$48.5 \pm 2.2$	$276.3 \pm 2.3$
S064	120.4957	22.9504	$-37.3 \pm 3.0$	$-17.1 \pm 2.0$	$41.0 \pm 2.8$	$245.4 \pm 2.2$

Note: I042, I045, LIUC, 0621, S010 and S064 are the data from Yu et al. (1997).

from 1990 to 1995 at stations I045, S010 and LIUC (Yu et al., 1997).

The numerical distinct-element models proposed by Hu et al. (1997, 2001) to account for the kinematics of anti-clockwise rotation of velocity field in SW Taiwan depend on three major factors: (1) the major faults and deformation front behaving as weak discontinuities; (2) the presence of the prominent Peikang High acting as a rigid indenter of the Chinese passive margin and (3) the presence of an offshore zone of mechanical weakness including the Manila trench and the related accretionary prism.

#### 4.1. The activity of the Chaochou Fault

In order to investigate the activity of the Chaochou Fault zone that trends N–S, we thus use both the E–W and N–S GPS components to characterize the fault-normal and fault-parallel kinematics, respectively. The results of this analysis are summarized in Figs. 4–6.

As Fig. 4 shows, the E–W components of station velocities relative to the stable shelf of the Taiwan Strait vary from  $-38.1 \pm 1.7$  mm/yr to  $-55.1 \pm 1.8$  mm/yr (the negative sign indicates westward motion). Remarkably, the absolute

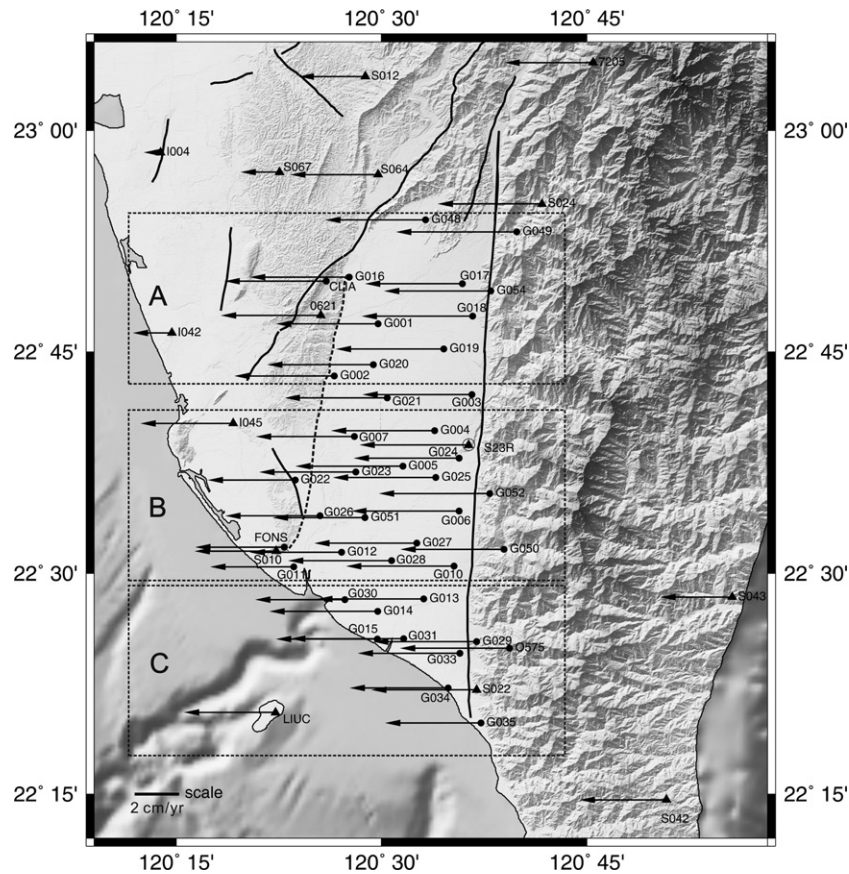


Fig. 4. E–W velocity components of GPS stations on the Pingtung plain relative to Paisha, Penghu, from 1996 to 1999. Same symbols as in Fig. 3.

values of station velocities gradually decrease from east to west, as the profiles of Fig. 5 shown. Most especially, there is no obvious contrast in velocity across the Chaochou Fault. As mentioned above, the Chaochou Fault is the major fault in the studied area and is considered as a steeply dipping thrust fault with a significant left-lateral movement.

We divided the whole study region into three subdomains (northern, central and southern) shown as rectangular frames A, B and C in Fig. 4. Our results indicate that the E–W velocity gradients of the GPS stations across the Chaochou Fault observed in three subdomains are not significant (Figs. 4 and 5). This result shows that the transverse component of motion across the Chaochou Fault, which was expected to be extensional according to geological analysis of fault zone evolution, is minor at present day. One should note, however, that our results reflect the deformation of the interseismic stage; because the possibility of major co-seismic motion of the Chaochou Fault is left open, these results should not be extrapolated to the long-term deformation.

As for the N–S components of station velocities in the study area (Fig. 6), the station velocities vary from  $2.1 \pm 2.0$  mm/yr to  $-18.8 \pm 1.7$  mm/yr (the negative sign indicates southward motion). Only nine stations (G052, G006, O575, G025, S23R, S024, S012, S022 and S064) show northward movement, with station velocities smaller than

2.1 mm/yr, and hence not significant. The other forty stations show southward movement with various velocity values. Remarkably, the southward station velocities are larger in the southwestern coastal area than in other regions. The maximum southward station velocity observed is  $18.8 \pm 1.7$  mm/yr. In detail, Fig. 6 shows that the increase in the N–S component of station velocities occurs in the NE–SW direction near the southwestern coast, rather than from North to South (compare for instance stations I045 and G034). For this reason, this aspect will be discussed in the next section, based on observation of NW and SE-directed components of motion. In any case, this general velocity pattern fits well with the hypothesis of lateral extrusion related to the ongoing ESE–WNW collision.

Examining the expected strike-slip, left-lateral component of motion along the Chaochou Fault, it appears that the present day gradients of N–S station velocities across the Chaochou Fault zone are minor and inconsistent in sense (Fig. 6). It should again be kept in mind that these 1996–1999 results do not preclude the possibility of large co-seismic motion occurring from time to time along the fault.

Based on the strike-slip and dip-slip components of GPS-derived station velocities, the Chaochou Fault should be considered as inactive during the 1996–1999 survey period. We infer that the Chaochou Fault may be locked with a strong mechanical coupling across the fault zone. However, the

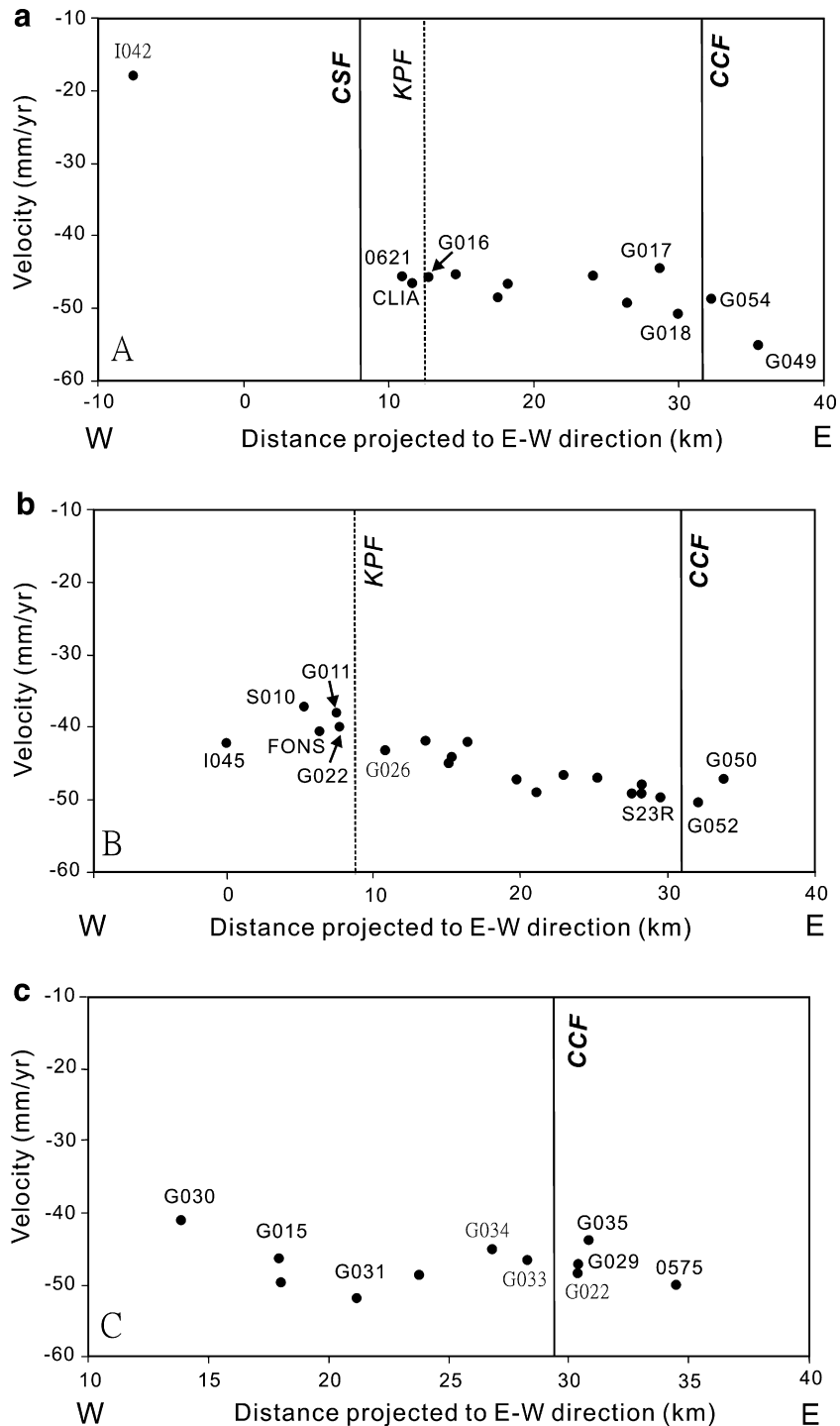


Fig. 5. Profiles of E–W components of station velocities along three subdomains of study area. CCF, Chaochou Fault; KPF, Kaoping Fault, CSF, Chishan Fault. Subdomains A, B and C are shown in Fig. 4.

absence of a dense network of GPS stations in the mountainous region east of the Chaochou Fault precludes further analysis in terms of possible locking depth and fault geometry.

#### 4.2. Activity of the Kaoping Fault

On the assumption of approximately rigid block limited by major structural discontinuities such as the Chaochou Fault, the inferred Kaoping Fault, the Chishan Fault and

the front thrust fault (i.e., deformation front), [Lacombe et al. \(2001\)](#) proposed the present-day kinematics of SW Taiwan is both undergoing the shorting and lateral escape. These authors took into account the fault-perpendicular and fault-parallel components of block motion deduced from the previous GPS data ([Yu et al., 1997](#)). They suggested the existence of left-lateral Kaoping Fault based on the change in azimuth of station velocities (S022, S23R in block 1 and 0621, LIUC, S010, I045 in block 2) across the

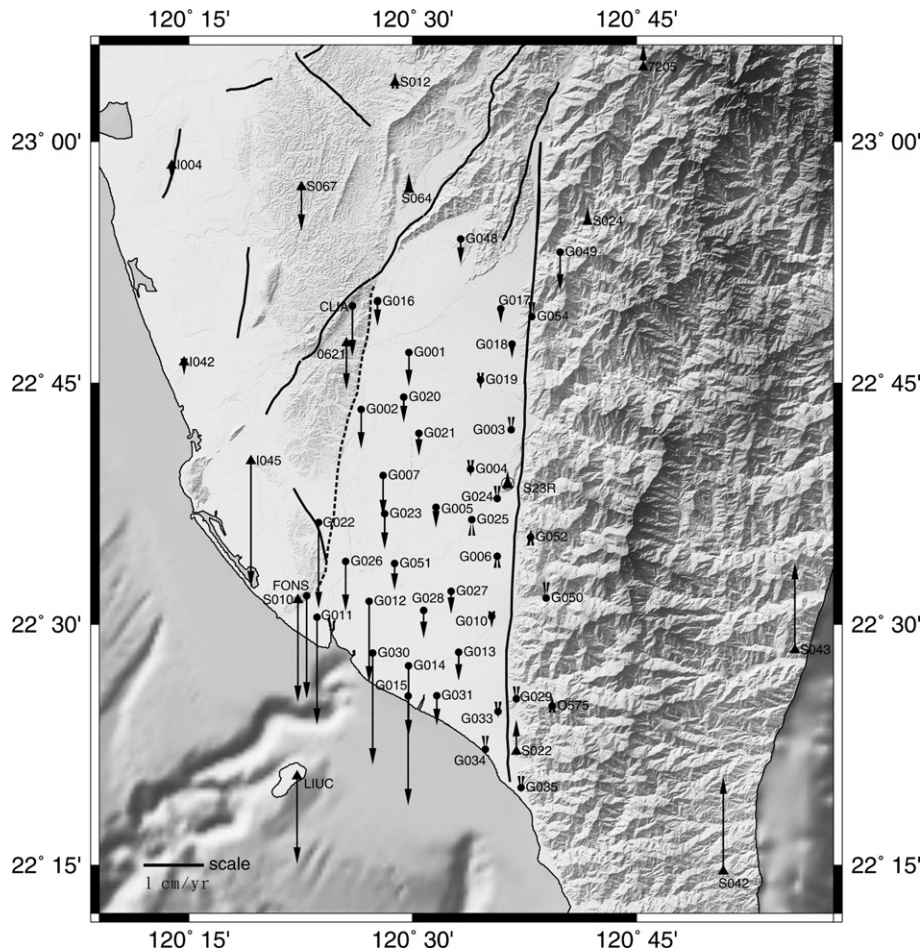


Fig. 6. N–S velocity components of GPS stations on the Pingtung plain relative to Paisha, Penghu, from 1996 to 1999. Same symbols as in Fig. 3.

fault. However, a major limitation in this approach resulted from the large spacing between the GPS stations, which were few at this time. We undertook a similar analysis with our denser network of GPS stations in the Pingtung–Kaohsiung area.

Considering the across-strike components first (Figs. 4 and 5), we plotted the E–W components of horizontal displacement because the trends of the Chaochou Fault and the inferred Kaoping Fault are nearly N–S (Fig. 2). Our results show the across-strike components are not significant with a value of less than  $\sim 5$  mm/yr by considering the velocity gradient of stations G011 and G026. If we consider the velocity gradient of stations in the northern part (CLIA, 0621 and G016) and the southern part (G022, G011 and G026) for the along-strike components of the Kaoping Fault, the left-lateral velocity increases southward from  $\sim 4$  mm/yr to  $\sim 8$  mm/yr based on geomorphological analysis. Shyu et al. (2005) proposed that the western side of the Pingtung plain is also a distinct topographic break (Fig. 2) and pointed out that this linear feature is likely to be modified by erosion of the Kaoping River, the major river of the Pingtung plain. Furthermore, the analysis of Holocene sediment thickness from the cores retrieved from the Pingtung plain suggest that pre-Quaternary rocks are more than 200 m lower in the basin located

at the east side of the Kaoping Fault than in the hills to the west (Shyu, 1999). This observation implies that the Kaoping Fault is a fault with at least several hundred meters of vertical slip, and separates the rocks of the hills from those of the basin. Contrary to the Chaochou Fault on the opposite edge of the Pingtung basin, where hard basement rocks crop out, the Kaoping Fault affects relatively soft formations of the Late Paleozoic on both its sides. As a consequence, the fault escarpment has undergone significant erosion by the Kaoping River and westward retreat, so that the present-day topography provides little evidence of fault scarp.

#### 4.3. Evidence of lateral extrusion

We further investigated the deformation pattern in the study area, in relation to the pattern of ESE–WNW collision. We accordingly decomposed the stations velocities into two components, plate-motion-perpendicular component (Figs. 7, 8) and the plate-motion-parallel-component (Figs. 9, 10). The direction of plate motion between the Philippine Sea plate and Eurasia is  $310^\circ$  based on the NUVEL-1 model (Seno et al., 1993). As a consequence, the two components considered display azimuths of  $040^\circ$  and  $130^\circ$ .

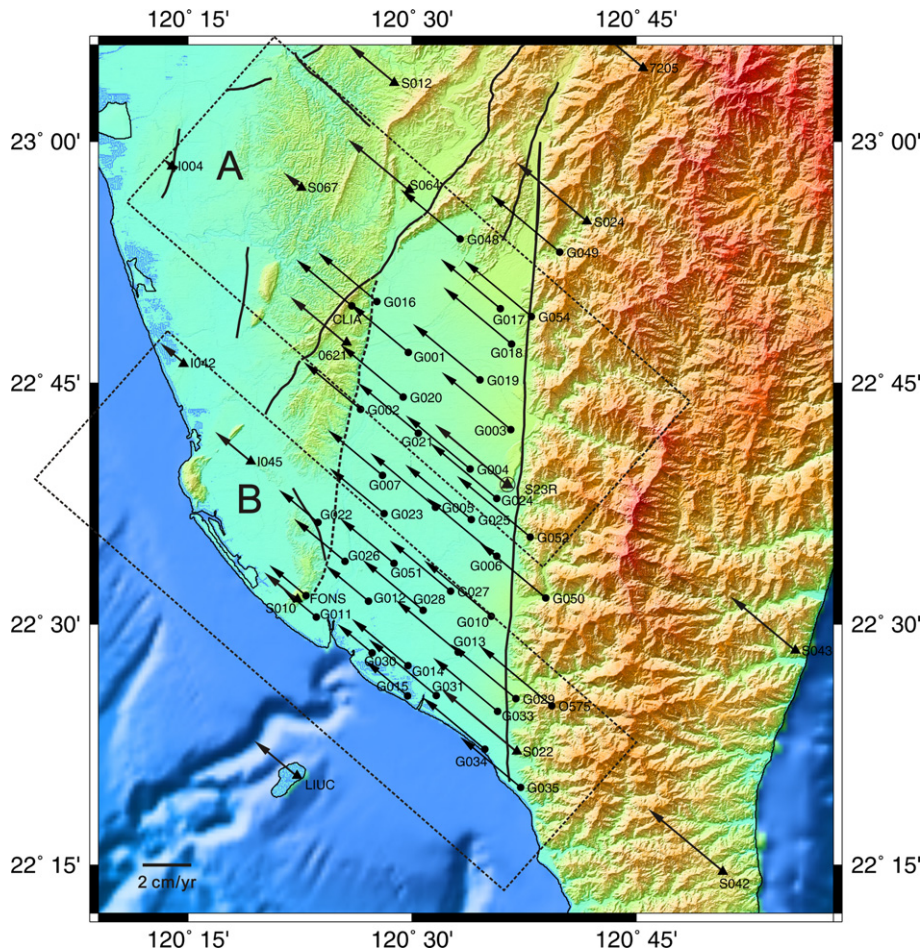


Fig. 7. Plate-motion-parallel components of GPS stations on the Pingtung plain relative to Paisha, Penghu (S01R), from 1996 to 1999. Dotted rectangles are the domains of the profiles. Symbols are the same as in Fig. 3.

This decomposition of station velocities also facilitated the investigation of activity of the Chishan Fault because of the trend of this fault is parallel or subparallel to the plate motion. Based on the plate-motion-parallel components, the station velocities decrease northwestward from 39.9 to 17.7 mm/yr (Figs. 7 and 8). An abrupt decrease apparently occurs around the Chishan Fault (Figs. 7 and 8, domain A) but the large spacing between stations precludes clearer identification of any velocity discontinuity. To the south, where the Chihshan Fault disappears near a zone of transfer faulting, the Fengshan transfer zone (Deffontaines et al., 1997), the station velocities decrease northwestward in a more gradual way. Taking the earlier IES stations into account (Yu et al., 1997), a significant difference in station velocity is located between stations S064 and S067 as well as between stations I042 and I045. Presently available GPS data thus allow identification of a SE–NW shortening of about 20 mm/yr and accommodated within an about 10-km-wide deformation zone.

Considering the plate-motion-perpendicular components (Figs. 9 and 10), the station velocities increase southwestward, from 28.7 to 44 mm/yr. An abrupt contrast in velocity apparently occurs across the southwest extension of the Chishan Fault zone near the coast (Figs. 9 and 10,

domain B), whereas to the north the change is smoother across the Chishan Fault itself (Figs. 9 and 10, domain B). This pattern of the plate-motion-perpendicular station velocities is consistent with the lateral extrusion that is expected to increase towards the southwest. However, there exists a strong possibility of a Chihshan Fault being locked in the interseismic stage, while motion occurs to the south along, and south of, the Fengshan transform fault zone.

The analogue models of Lu and Malavieille (1994) also suggested a southward lateral extrusion of the southern Western Foothills in response to the oblique collision between the Philippines Sea plate and Eurasian plate. Based on numerical simulations, Hu et al. (1997, 2001) pointed out that the significant counter-clockwise rotations of station velocities on the coastal area of the Pingtung plain is a result of lateral extrusion. Our results clearly demonstrate that the transtensional deformation and the plate-motion-normal variation of southwestward increase of extensional deformation in the whole area of the Pingtung plain. Based on Quaternary paleostress analysis (Lacombe et al., 1999, 2001), the significant southward increase in the occurrence of extension features which corresponds most nearly with the N–S extension during last stage of fold development. They pointed out that the tectonic escape might result from

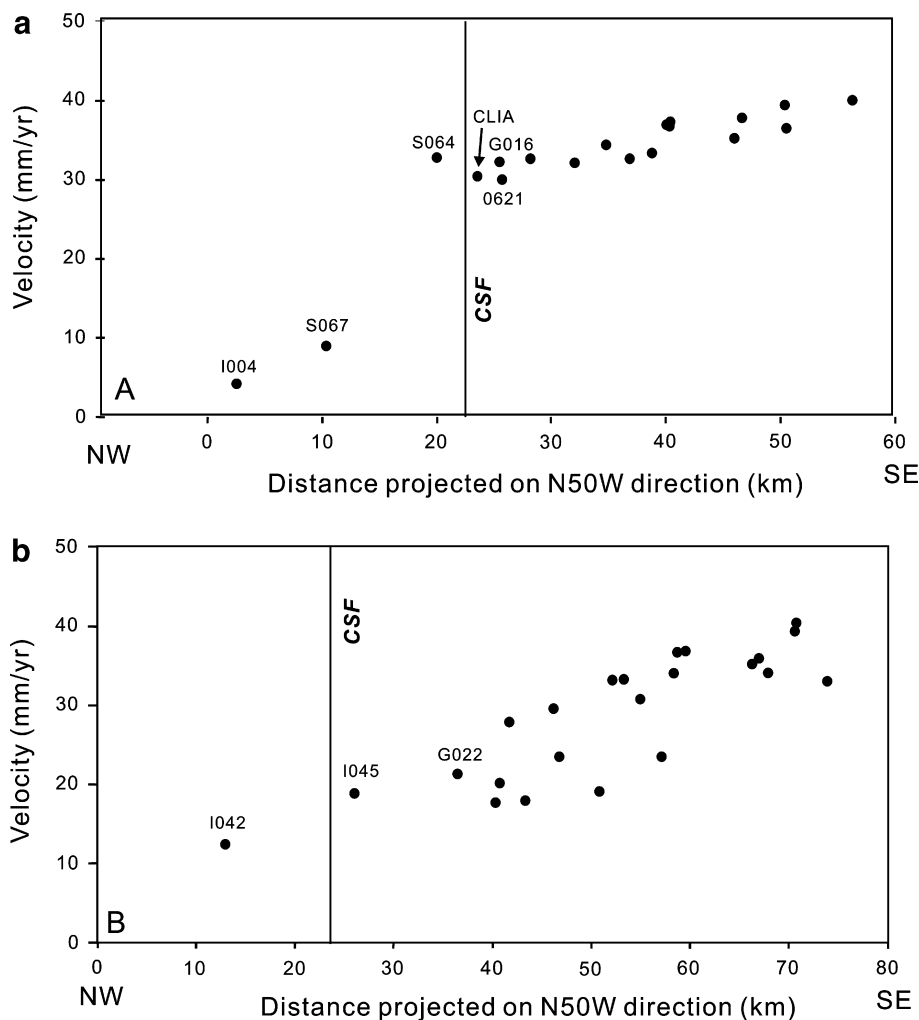


Fig. 8. Plate-motion-parallel components of station velocities along two profiles of the study area. CSF, Chishan Fault. Domains of profiles A, and B are shown in Fig. 7.

the decreasing of a N–S confinement during the last E–W shortening in Pleistocene.

Based on the inversion of fault slip and continuous deformation deduced from GPS data in Taiwan (Yu et al., 1997), Bos et al. (2003) also presented a surface deformation model for southern Taiwan. This model exhibited a strain pattern with E–W contraction accompanied by a southward increase of predominantly N–S oriented extension. They found a right-lateral thrust motion of  $\sim 14$  mm/yr in a N54°W direction in the deformation front zone, and a left-lateral normal motion of 6–13 mm/yr in the a N110°–130°E direction in the Chaochou Fault zone. The major block bounded by these faults is subject to counter-clockwise rotation at a rate of about 12.5°/Ma (Bos et al., 2003), whereas the areas east and west of this block are undergoing significantly smaller counter-clockwise rotation rates, or even clockwise rotation. The authors suggested these patterns of surface deformation are indicative of lateral extrusion toward the Manila accretionary wedge south of Taiwan. Our results of plate-motion-normal component (Figs. 9 and 10), the right-lateral strike-slip motion along the Chishan Fault in domains A, is  $\sim 7$  mm/yr by taking two

adjacent stations S064 and CLIA (Fig. 10a) across the fault into account. However, if we take I045 and I042 into account (Fig. 10b), the right-lateral shear across the fault is larger,  $\sim 30$  mm/yr. It implies that the other active structures with right-lateral motion between these two stations may accommodate the right-lateral shear.

Based on the results of geodetic re-triangulation of 1914–1979 (Chen, 1984), land subsidence prevails on the coastal area of the Pingtung plain. The maximum subsidence rate is  $\sim 30$  mm/yr. This significant subsidence may partly result from the prominent groundwater level decrease for aquacultural use. However, in a recent study of the withdrawal of groundwater, Kuo et al. (2001) pointed that long-term observation of the groundwater table in this region either dropped or showed little change over the last decade and suggested that the total subsidence of the southern Pingtung plain may be the result of a combination of region tectonic tilting and local over-withdrawal groundwater. These observations are also consistent with the Holocene subsidence patterns estimated from the drilling cores in the Pingtung plain (Lai et al., 2002). However, the average long-term subsidence rate is  $\sim 4$  mm/yr. And this

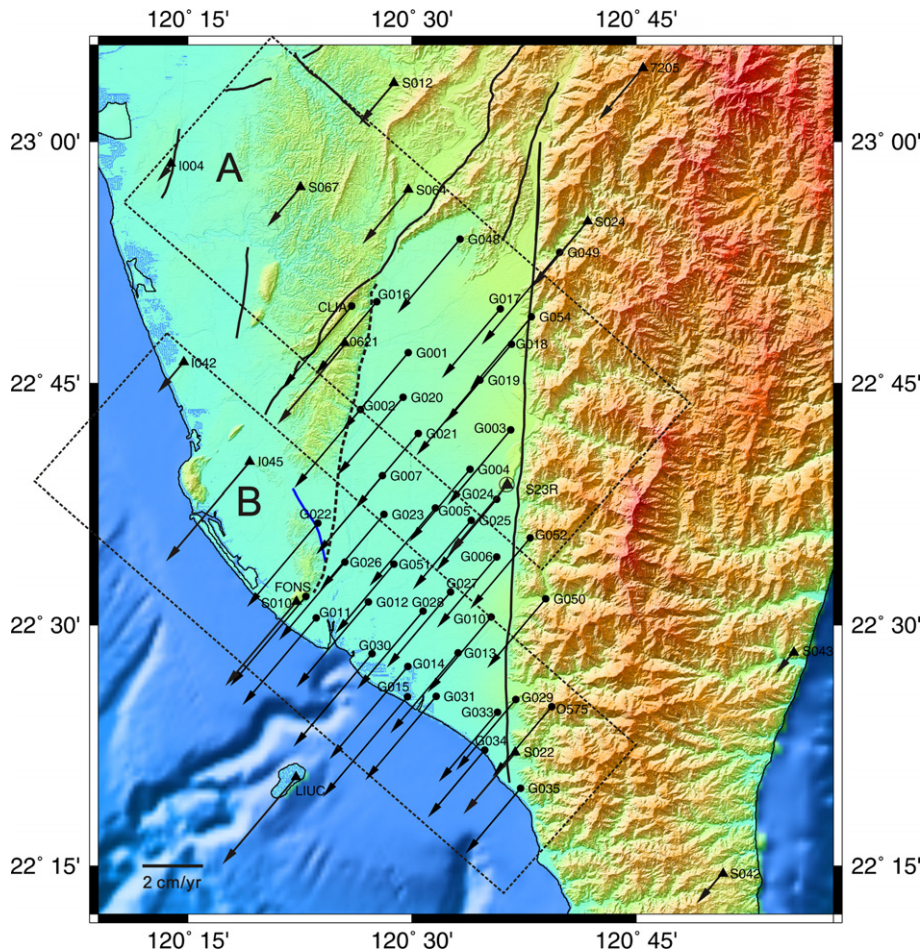


Fig. 9. Plate-motion-normal components of GPS stations on the Pingtung plain relative to Paisha, Penghu (S01R) from 1996 to 1999. Dotted rectangles are the domains of the profiles (See Fig. 10). Symbols are the same as Fig. 3.

long-term average subsidence rate from Holocene in southern Pingtung plain is much smaller than the observation derived by GPS measurements from 1996 to 1999 (Hu et al., 2006). We infer that this regional subsidence results from both the prominent groundwater level decrease along with rapid subsidence in the coastal region of the Pingtung plain and the transtensional deformation associated with the tectonic extrusion.

## 5. Discussion

Four years of GPS measurements of the Pingtung–Kaohsiung network and the “Taiwan GPS Network” have provided the complete velocity field depiction in SW Taiwan relative to the stable continental shelf. The dense GPS network facilitates the detailed verification of a tectonic model of SW Taiwan. Our results are in general agreement with the previous models of lateral extrusion due to the low lateral confining conditions related to the Manila subduction zone as a free boundary or/and the presence of prominent Peikang High as a rigid indenter (Lu and Malavieille, 1994; Lu et al., 1998; Hu et al., 1997, 2001; Lacombe et al., 1999, 2001; Bos et al., 2003). Based on the rigid blocks models (Angelier et al., 1999; Lacombe

et al., 2001), the escaping area comprises four rigid blocks moving toward the SW along major discontinuities with both the lateral and reverse shear. These discontinuities comprise the right-lateral reverse motion of the Deformation Front, right-lateral reverse motion of the Chishan Fault, left-lateral reverse motion of the Kaoping Fault and left-lateral reverse motion of the Chaochou Fault. Within the regional scale, Bos et al. (2003) estimated the velocity gradient field and fault slip rate of the major discontinuities by using the inversion method on the basis of 141 GPS data in the Taiwan area (Yu et al., 1997). They found the right-lateral thrust motion of  $\sim 14$  mm/yr in a  $N54^\circ W$  direction along the Deformation Front and left-lateral normal motion of 6–13 mm/yr in a direction of  $N110^\circ$ – $N130^\circ E$  along the Chaochou–Chishan Fault. These predictions suggest the left-lateral motion or left-lateral motion along the Chaochou Fault; however, our results clearly show the insignificant motion along the Chaochou Fault on the basis of both across-strike and along-strike components of GPS data. The disagreement of observation is due to the data density of different GPS networks. The previous GPS data (Yu et al., 1997) are not sufficient to determine the fault slip of the Chaochou Fault if we only consider the difference in direction and

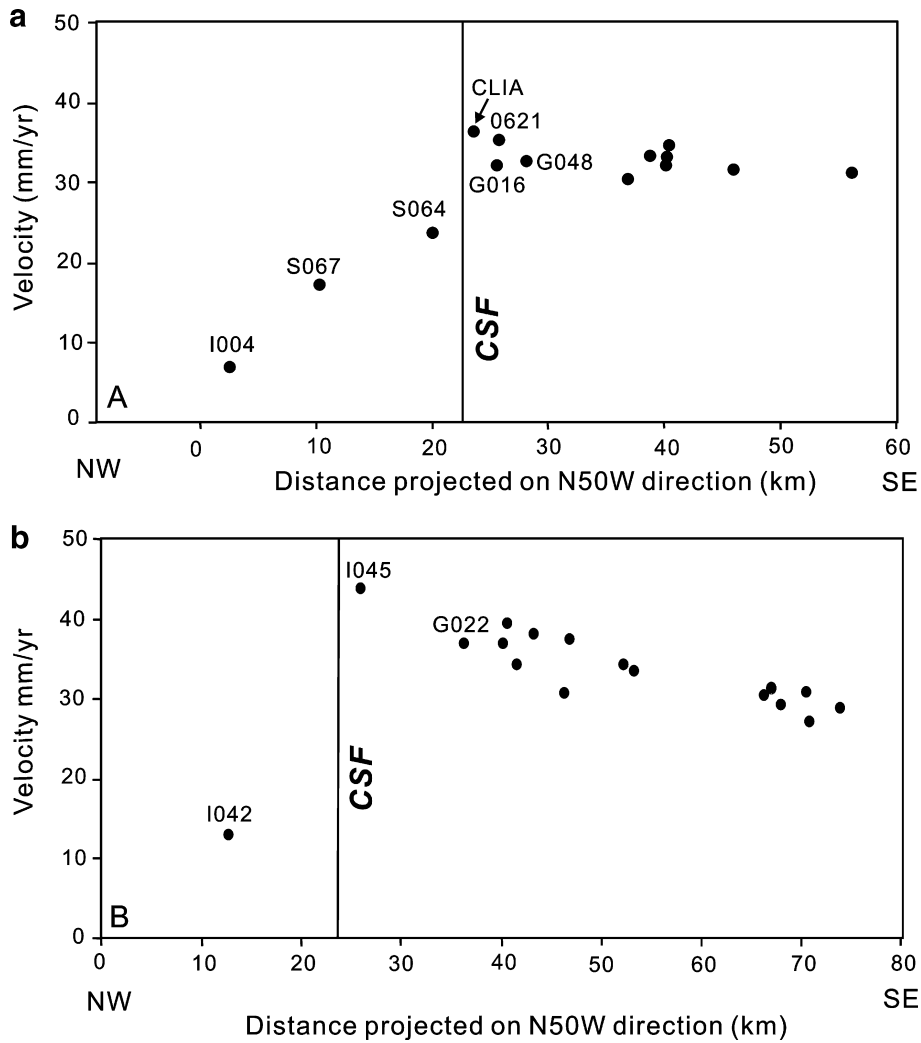


Fig. 10. Plate-motion-normal components of station velocities along two profiles of the study area. CSF, Chishan Fault. Domains of profiles A and B shown in Fig. 9.

magnitude of motion between station S043 and S23R across the whole Slate Belt. We imply that the left-lateral normal motion should accommodate in the Slate Belt. Fisher et al. (2002) pointed out that the southern Backbone Range records extension perpendicular to the mountain belt, and oblique strain axes in the eastern Backbone Range are consistent with left-lateral shear.

One question needs to be addressed clearly about the time and scale of the lateral extrusion in SW Taiwan. Based upon analogue modeling (Lu et al., 1998), predicted the lateral extrusion is mainly produced by Peikang High and could result in a large left-lateral transfer zone around the shelf break of the Chinese continental margin. Lacombe et al. (2001) proposed a different model and suggested that the lateral extrusion is acting on the southern tip of the collision belt, probably south of the Chishan Transfer Fault Zone (CTFZ, for detail see Defontaine et al., 1997). However, geological observations in SW Taiwan do not show clear evidence of lateral extrusion in the strata of Quaternary formation (Lacombe et al., 1999). This implies that the lateral extrusion process must have

developed recently and compatible with the young and ongoing collision in southern Taiwan. They also pointed out the escaping blocks move southwestward to offshore area based on the similar trend of velocity vectors of LIUC, S010, G011, G030 and G015 (Fig. 3). However, the marine morphology and seismic profiles offshore in SW Taiwan also provides no conclusive evidence for tectonic escape (Liu et al., 1997). Indeed, the most recent GPS measurements indicate the velocity field in SW Taiwan (Yu et al., 1997) and in our study area seems to have a systematic trend of increasing southwestward components as a prominent phenomenon of lateral extrusion in SW Taiwan. On the basis of the inversion of BATS (Broadband Array in Taiwan for Seismology) data, Kao and Jian (2001) suggested that the lateral extrusion is probably only a secondary feature in the tectonic processes of Taiwan by two shallow events occurring in SW Taiwan. It is worthy of notice that one strike-slip event at a depth of 24 km with *P*-axis in the NE–SE direction is a significant indicator that significant shear motion of at least crustal scale exists. Yeh et al. (1991) also pointed out the

right-lateral motion along NE-trending structures, especially along the frontal thrust zone and the Chishan Fault zone, but the focal depths are not precisely constrained. The significance of counter-clockwise of station velocities is greatly different to those located within the inner part of mountain belt. These observations imply that in the case of SW Taiwan the velocity vectors may reflect the movement of the sedimentary cover and are at least partially decoupled from the deeper crust.

## 6. Conclusions

In summary, the dense GPS network in the Pingtung area shows detailed kinematic behavior of lateral extrusion of the transition zone between collision mountain belt and accretionary prisms of the subduction zone. The distinctive counter-clockwise rotation of the velocity vectors across the Kaohsiung–Pingtung area of SW Taiwan can probably be best explained as a result of the lateral extrusion. Our results clearly demonstrate the transtensional deformation and the along-strike variation of southward increase of extensional deformation in the whole area of southwest Taiwan. The Pingtung plain characterizes the rapid subsidence basin between the Central Range and Western Foothills. The right-lateral and left-lateral structures facilitate the southwestward extrusion and the deformation of the Western Foothills indicates N–S stretching and E–W shortening. Moreover, GPS vectors indicate that the Chishan Fault is dominated by right-lateral motion with a fault slip rate  $\sim 7$  mm/yr in the N50°W direction. The Kaoping Fault bounded on the west side of the Pingtung plain is dominated by left-lateral motion with a  $\sim 4$ –8 mm/yr in the N–S direction. It is noteworthy that the significant right-lateral component of motion of  $\sim 24$ –30 mm/yr should be accommodated on the active structures west of the Chishan Fault between the coast and the deformation front. The right-lateral and left-lateral structures facilitate the southwestward extrusion. The Chaochou Fault is the major fault in the studied area and is considered as the thrust fault with left-lateral movement. Based on our studies, the velocity gradients of the GPS stations across the Chaochou Fault are not significant. This implies that the Chaochou Fault is locked and the mechanical coupling along the fault plane should be very strong. The maximum subsidence rate is about  $\sim 30$  mm/yr near the coastal area of southeastern part of Pingtung plain. We infer this regional subsidence maybe due to both the prominent groundwater level decrease with rapid subsidence in the coastal of Pingtung plain as well as the transtensional deformation associated with the tectonic extrusion.

## Acknowledgements

We benefited from fruitful discussions with Jacques Angelier, Chia-Yu Lu, Hao-Tsu Chu, Jian-Cheng Lee, Meng-Long Hsieh, Erwan Pathier and Benoit Deffontaines.

This research was supported by National Science Council of Taiwan grant (NSC93-2116-M-002-008, 94-2119-M-002-008) and the Central Geological Survey of the MOEA. Some figures were made using the GMT software written by Paul Wessel and Walter H.F. Smith (1998).

## References

- Angelier, J., 1986. Preface. Geodynamics of the Eurasia–Philippine Sea plate boundary. *Tectonophysics* 125, IX–X.
- Angelier, J., Yu, S.-B., Lee, J.-C., Hu, J.-C., Chu, H.-T. 1999. Active deformation of Taiwan collision zone: discontinuities in GPS displacement field. In: Workshop International Conference and 4th Sino-French Symposium on Active Subduction and Collision in Southeast Asia, *Memoires Geosciences-Montpellier*, N° 14, Program and extended abstracts, pp. 287–290.
- Angelier, J., Chu, H.-T., Lee, J.-C., Hu, J.-C., 2000. Active faulting and earthquake risk: the Chihshang fault case, Taiwan. *Journal of Geodynamics* 29, 151–185.
- Angelier, J., Lee, J.-C., Chu, H.-T., Hu, J.-C., Lu, C.-Y., Chan, Y.-C., Lin, T.-J., Font, Y., Deffontaines, B., Tsai, Y.-B., 2001. Le Séisme de Chichi (1999) et sa place dans l'orogène de Taiwan. *Comptes Rendus de l'Académie des Sciences Paris, Sciences de la Terre et des Planètes* 333, 5–21.
- Bonilla, M.G. A review of recently active fault in Taiwan, USGS open-file report 75-41, 1975, pp. 1–55.
- Bonilla, M.G., 1977. Summary of Quaternary faulting and elevation changes in Taiwan. *Geological Society of China Memoir* 2, 43–56.
- Bos, A.G., Spakman, W., Nyst, M.C.J., 2003. Surface deformation and tectonic setting of Taiwan inferred from a GPS velocity field. *Journal of Geophysical Research* 108 (B10), 2458. doi:10.1029/2002JB002336.
- Byrne, T., Crespi, J. 1997. Kinematics of the Taiwan arc-continent collision and implications for orogenic process, In: International Conference and Sino-American Symposium on Tectonics of East Asia, Taipei, Taiwan, p. 38.
- Chai, B.H.T., 1972. Structure and tectonic evolution of Taiwan. *American Journal of Science* 272, 389–422.
- Chan, Y.-C., Lu, C.-Y., Lee, J.-C. 2000. Orogen-parallel shearing in ongoing mountain building: a case study from the southeastern central range of Taiwan, EOS, *Transactions American Geophysical Union*, Fall Meeting Abstract, 81 (48).
- Chen, H.-F., 1984. Crustal uplift and subsidence in Taiwan: an account based on retriangulation results, Special Publication of the Central Geological Survey 3, 127–140 (in Chinese).
- Chen, Y.-G., Liu, T.-K., 2000. Holocene uplift and subsidence along an active tectonic margin southwestern Taiwan. *Quaternary Science Reviews* 19, 923–930.
- Chiang, C.-S., Yu, H.-S., Chou, Y.-W., 2004. Characteristics of the wedge-top depozone of the southern Taiwan foreland basin system. *Basin Research* 16, 65–78. doi:10.1111/j.1365-2117.2003.00222.x.
- Dadson, S.J., Hovius, N., Chen, H., Dade, W.B., Hsieh, M.-L., Willett, S.D., Hu, J.-C., Horng, M.-J., Chen, M.-C., Stark, C.P., Lague, D., Lin, J.-C., 2003. Links between erosion, runoff variability, and seismicity in the Taiwan orogen. *Nature* 426, 648–651.
- Deffontaines, B., Lacombe, O., Angelier, J., Mouthereau, F., Lee, C.-T., Deramond, J., Lee, J.-F., Yu, M.-S., Liu, P.-M., 1997. Quaternary transfer faulting in Taiwan foothills: evidence from a multisource approach. *Tectonophysics* 274, 61–82.
- Dixon, T.H., 1991. An introduction to the global positioning system and some geological applications. *Reviews of Geophysics* 29, 249–276.
- Fisher, D.M., Lu, C.-Y., Chu, H.-T. 2002. Taiwan Slate Belt: insights into the ductile interior of an arc-continent collision. In: Byrne, T.B., Liu, C.-S. (Eds.), *Geology and Geophysics of an Arc-Conti-*

- nent Collision, Taiwan. The Geological Society of America Special Paper 358, pp. 93–106.
- Hickman, J.B., Wiltchko, D.V., Hung J.-H., Fang, P., Bock, Y. 2002. Structure and evolution of the active fold-and-thrust belt of southwestern Taiwan from Global Positioning System analysis. In: Byrne, T.B., Liu, C.-S., (Eds), *Geology and Geophysics of an Arc-Continent Collision, Taiwan*. The Geological Society of America Special Paper 358, pp. 93–106.
- Ho, C.-S., 1986. A synthesis of the geological evolution of Taiwan. *Tectonophysics* 125, 1–16.
- Hovius, N., Stark, C.P., Chu, H.-T., Lin, J.-C., 2000. Supply and removal of sediment in a landslide-dominated mountain belt: Central Range, Taiwan. *The Journal of Geology* 108, 73–89.
- Hsu, T.-L., Chang, H.-C., 1979. Quaternary faulting in Taiwan. *Geological Society of China Memoir* 3, 155–165.
- Hu, J.-C., Angelier, J., 1996. Modelling of stress-deformation relationship in a collision belt. Taiwan. *Terrestrial, Atmospheric and Oceanic Sciences* 7 (4), 447–465.
- Hu, J.-C., Angelier, J., Lee, J.-C., Chu, H.-T., Byrne, D., 1996. Kinematics of convergence, deformation and stress distribution in the Taiwan collision area: 2-D finite-element numerical modelling. *Tectonophysics* 255, 243–268.
- Hu, J.-C., Angelier, J., Yu, S.-B., 1997. An interpretation of the active deformation of southern Taiwan based on numerical simulation and GPS studies. *Tectonophysics* 274, 145–169.
- Hu, J.-C., Yu, S.-B., Angelier, J., Chu, H.-T., 2001. Active deformation of Taiwan from GPS measurements and numerical simulations. *Journal of Geophysical Research* 106, 2265–2280.
- Hu, J.-C., Yu, S.-B., Chu, H.-T., Angelier, J. 2002. Transition tectonics of northern Taiwan induced by convergence and trench retreat. In: Byrne, T.B., Liu, C.-S., (Eds), *Geology and Geophysics of an Arc-Continent Collision, Taiwan*. The Geological Society of America Special Paper 358, pp. 147–160.
- Hu, J.-C., Chu, H.-T., Hou, C.-S., Chen, R.-F., Lai, T.-H., Nien, P.-F., 2006. The contribution to tectonic subsidence by groundwater abstraction in the Pingtung area, southwestern Taiwan as determined by GPS measurements. *Quaternary International* 147, 62–69.
- Hugentobler U., Schaer S., Fridez P., 2001. Bernese GPS software, Version 4.2. Astronomical Institute, University of Berne, 515 pp.
- Kao, H., Jian, P.-R., 2001. Seismogenic patterns in the Taiwan region: insights from source parameter inversion of BATS data. *Tectonophysics* 333, 179–198.
- Kuo C.-H., Chan Y.-C., Wang C.-H., 2001. Subsidence: over withdrawal groundwater, tectonic or both? EOS Transactions American Geophysical Union, Fall Meeting, Abstract 82 (47) (Suppl.), F479.
- Lacombe, O., Mouthereau, F., Deffontaines, B., Angelier, J., Chu, H.-T., Lee, C.-T., 1999. Geometry and Quaternary kinematics of fold-and-thrust units of southwestern Taiwan. *Tectonics* 18, 1198–1223.
- Lacombe, O., Mouthereau, F., Angelier, J., Deffontaines, B., 2001. Structural, geodetic and seismological evidence for tectonic escape in SW Taiwan. *Tectonophysics* 333, 323–345.
- Lai, T.-H., Hsieh, M.-L., Liew, P.-M., Chen, Y.-G. 2002. Holocene rock uplift and subsidence in the coastal area of Taiwan. EOS, Transactions American Geophysical Union, Fall Meeting Abstract, 83(47), F1280.
- Li, Y.-H., 1976. Denudation of Taiwan island since the Pliocene epoch. *Geology* 4, 105–107.
- Liew, P.-M., Hsieh, M.-L., Lai, C.-K., 1990. Tectonic significance of holocene marine terraces in the coastal range, eastern Taiwan. *Tectonophysics* 183, 121–127.
- Lin, A.T., Watts, A.B., 2002. Origin of the west Taiwan basin by orogenic loading and flexure of a rifted continental margin. *Journal of Geophysical Research* 107, 2185–2203.
- Lin, C.-W., Chang, H.-C., Lu, S.-T., Shih, T.-S., Huang, W.-J., 2000. An introduction of the active faults of Taiwan. Special Publication of the Central Geological Survey 13, 122 pp.
- Liu, C.-C., Yu, S.-B., 1990. Vertical crustal movements in eastern Taiwan and their tectonic implications. *Tectonophysics* 183, 111–119.
- Liu, C.S., Huang, I.L., Tseng, L.S., 1997. Structural features of southwestern Taiwan. *Marine Geology* 137, 305–319.
- Liu, T.-K., Hsieh, S., Chen, Y.-G., Chen, W.-S., 2001. Thermo-kinematic evolution of the Taiwan oblique-collision mountain belt as revealed by zircon fission track dating. *Earth and Planetary Science Letters* 186, 45–56.
- Lu, C.-Y., Malavieille, J., 1994. Oblique convergence, indentation and rotation tectonics in the Taiwan mountain belt: insights from experimental modeling. *Earth and Planetary Science Letters* 121, 477–494.
- Lu, C.-Y., Jeng, F.-S., Chang, K.-J., Jian, W.-T., 1998. Impact of basement high on the structure and kinematics of western Taiwan thrust wedge: insights from sandbox models. *Terrestrial, Atmospheric and Oceanic Sciences* 9 (3), 533–550.
- Lundberg, N., Reed, D.L., Liu, C.-S., Lieske, J., 1997. Forearc-basin closure and arc accretion in submarine suture zone south of Taiwan. *Tectonophysics* 274, 5–23.
- Malavieille, J., Lallemand, S.E., Dominiquez, S., Deschamps, A., Lu, C.-Y., Liu, C.-S., Schnürle, P., 2002. Arc-continent collision in Taiwan: new marine observations and tectonic evolution. In: Byrne, T.B., Liu, C.-S., (Eds), *Geology and Geophysics of an Arc-Continent Collision, Taiwan*. The Geological Society of America Special Paper 358, pp. 187–211.
- Molnar, P., Tapponnier, P., 1978. Active tectonics of Tibet. *Journal of Geophysical Research* 83, 5361–5375.
- Mouthereau, F., Deffontaines, B., Lacombe, O., Angelier, J., 2002. Variation along the strike of the Taiwan thrust belt: basement control on structural style, wedge geometry, and kinematics. In: Byrne, T.B., Liu, C.-S. (Eds.), *Geology and Geophysics of an Arc-Continent Collision, Taiwan*. The Geological Society of America Special Paper 358, pp. 31–54.
- Pirazzoli, P.A., Arnold, M., Giresse, P., Hsieh, M.-L., Liew, P.-M., 1993. Marine deposits of late glacial times exposed by tectonic uplift on the east coast of Taiwan. *Marine Geology* 110, 1–6.
- Ratschbacher, L., Frisch, W., Linzer, H.-G., Merle, O., 1991. Lateral extrusion in the eastern Alps, part 2: structural analysis. *Tectonics* 10 (2), 257–271.
- Segall, P., Davis, J.L., 1997. GPS applications for geodynamics and earthquake studies. *Annual Reviews of Earth Planetary Sciences* 25, 301–336.
- Seno, T., Stein, S., Gripp, A.E., 1993. A model for the motion of the Philippine Sea plate consistent with NUVEL-1 and geological data. *Journal of Geophysical Research* 98, 17941–17948.
- Shyu, J.B.H., 1999. The sedimentary environment of southern Pingdong plain since the last glacial, Master Thesis, National Taiwan University, Taipei, pp. 212.
- Shyu, J.B.H., Sieh, K., Chen, Y.-G., Liu, C.-S., 2005. Neotectonic architecture of Taiwan and its implications for future large earthquakes. *Journal of Geophysical Research* 110, B08402. doi:10.1029/2004JB003251.
- Suppe, J., 1984. Kinematics of arc-continent collision, flipping of subduction and back-arc spreading near Taiwan. *Geological Society of China Memoir* 6, 21–33.
- Tapponnier, P., Peltzer, A., Le Dain, Y., Armijo, R., Cobbold, P., 1983. Propagation extrusion tectonics in Asia: new insights from simple experiments with plasticine. *Geology* 10, 611–616.
- Teng, L.S., 1990. Geotectonic evolution of late Cenozoic arc-continent collision in Taiwan. *Tectonophysics* 183, 57–76.
- Teng, L.S., 1996. Extensional collapse of the northern Taiwan mountain belt. *Geology* 10, 949–952.
- Tsai, Y.-B., 1986. Seismotectonics of Taiwan. *Tectonophysics* 125, 17–37.
- Vita-Finzi, C., 2000. Deformation and seismicity of Taiwan. *Proceedings of the National Academy of Sciences* 97, 11176–11180.
- Wang, C.-H., Burnett, W.C., 1990. Holocene mean uplift rates across an active plate collision boundary in Taiwan. *Science* 248, 204–206.
- Wessel, P., Smith, W.H.F., 1998. New, improved version of the generic mapping tools released. EOS Transactions American Geophysical Union 79, 579.
- Yeh, Y.-H., Barrier, E.C.-H., Lin, C.-H., Angelier, J., 1991. Stress tensor analysis in the Taiwan area from focal mechanisms of earthquakes. *Tectonophysics* 200, 267–280.
- Yu, S.-B., Chen, H.-Y., 1994. Global positioning system measurements of crustal deformation in the Taiwan arc-continent collision zone. *Terrestrial, Atmospheric and Oceanic Sciences* 5, 477–498.

- Yu, S.-B., Chen, H.-Y., Kuo, L.-C., 1997. Velocity field of GPS stations in the Taiwan area. *Tectonophysics* 274, 41–59.
- Yu, S.-B., Kuo, L.-C., Punongbayan, R.S., Ramos, E.G., 1999. GPS observation of crustal deformation in the Taiwan-Luzon region. *Geophysical Research Letters* 26, 923–926.
- Yu, S.-B., Kuo, L.-C., 2001. Present-day crustal motion along the longitudinal valley fault, eastern Taiwan. *Tectonophysics* 333, 199–217.
- Zang, S.-X., Chen, Q.-Y., Ning, J.-Y., Shen, Z.-K., Liu, Y.-G., 2002. Motion of the Philippine sea plate consistent with the NUVEL-1A model. *Geophysical Journal International* 150, 809–819.